CD81 gene defect in humans disrupts CD19 complex formation and leads to antibody deficiency

Menno C. van Zelm,[1] Julie Smet,[2] Brigitte Adams,[3] Françoise Mascart,[2] Liliane Schandené,[2] Françoise Janssen,[3] Alina Ferster,[4] Chiung-Chi Kuo,[5] Shoshana Levy,[5] Jacques J.M. van Dongen,[1] and Mirjam van der Burg[1]

[1]Department of Immunology, Erasmus MC, University Medical Center, Rotterdam, Netherlands.
[2]Immunobiology Clinic and Laboratory of Vaccinology and Mucosal Immunity, Hôpital Erasme, Université Libre de Bruxelles, Brussels, Belgium.
[3]Department of Nephrology and [4]Department of Hemato-oncology and Immunology, HUDERF, Université Libre de Bruxelles.
[5]Division of Oncology, Department of Medicine, Stanford University School of Medicine, California.

Antibody deficiencies constitute the largest group of symptomatic primary immunodeficiency diseases. In several patients, mutations in *CD19* have been found to underlie disease, demonstrating the critical role for the protein encoded by this gene in antibody responses; CD19 functions in a complex with CD21, CD81, and CD225 to signal with the B cell receptor upon antigen recognition. We report here a patient with severe nephropathy and profound hypogammaglobulinemia. The immunodeficiency was characterized by decreased memory B cell numbers, impaired specific antibody responses, and an absence of CD19 expression on B cells. The patient had normal *CD19* alleles but carried a homozygous *CD81* mutation resulting in a complete lack of CD81 expression on blood leukocytes. Retroviral transduction and glycosylation experiments on EBV-transformed B cells from the patient revealed that CD19 membrane expression critically depended on CD81. Similar to CD19-deficient patients, CD81-deficient patients had B cells that showed impaired activation upon stimulation via the B cell antigen receptor but no overt T cell subset or function defects. In this study, we present what we believe to be the first antibody deficiency syndrome caused by a mutation in the *CD81* gene and consequent disruption of the CD19 complex on B cells. These findings may contribute to unraveling the genetic basis of antibody deficiency syndromes and the nonredundant functions of CD81 in humans.

Introduction

Antibody deficiencies form the largest group of primary immunodeficiencies. Patients can present either in early childhood or in adulthood with increased susceptibility to infections, which are mainly caused by encapsulated bacteria. Initial diagnosis and subdivision into 3 categories is based on the reduction of serum antibody levels in combination with the number of B cells in peripheral blood (1, 2): (a) patients with strongly reduced B cell numbers and serum Ig levels are defined as agammaglobulinemic; (b) patients with normal B cell numbers, normal to high IgM, but severely reduced IgG and IgA have a hyper-IgM syndrome; (c) patients with low to normal B cell numbers and strongly reduced levels of IgG and of IgA or IgM are diagnosed with a common variable immunodeficiency disorder (CVID). In the last 2 decades, multiple gene defects have been identified that underlie these types of antibody deficiencies (2, 3). In the majority of patients diagnosed with agammaglobulinemia or a hyper-IgM syndrome, the underlying genetic defect has been identified (2). Whereas mutations have been described in patients diagnosed with CVID (4–9), in more than 90% of these patients, no associated genetic defect has been found. Early diagnosis is necessary to prevent high incidence of bronchitis and pneumonia, which often lead to chronic lung disease. Current treatment protocols involving gammaglobulin replacement therapy and prophylactic antibiotics are quite successful in limiting severe infections. Still, the clinical heterogeneity and high frequency of autoimmune diseases and malignancies in CVID patients warrants the identification of immunological and genetic defects to support proper treatment and prevention of irreversible organ damage (10–13).

Recent studies have identified mutations in *CD19* as underlying an antibody deficiency syndrome resembling CVID (5, 6). On mature B cells, CD19 is mainly present in a complex together with CD21, CD81, and CD225 (14). This CD19 complex signals in conjunction with the B cell antigen receptor (BCR), thereby decreasing the threshold for BCR-dependent signaling (15, 16). CD19 and complement receptor CD21 both have a single transmembrane domain and bind each other directly (17, 18). Because CD21 lacks intracellular domains, it is thought that CD21 signals via CD19, which has multiple tyrosine residues involved in signaling processes (19). Whereas CD19 and CD21 are quite specifically expressed on B cells, CD81 and CD225 are widely expressed on immune cells (T, B, and NK lymphocytes, monocytes, and eosinophils), hepatocytes, and most stromal and epithelial cells (20).

The function of tetraspanin CD81 has been carefully studied in 3 independently generated CD81-knockout mouse models (21–23). The most prominent observations made were reduced CD19 expression on mature B cell and impaired B cell activation and antibody production in response to T cell–dependent antigens (21–23). Whereas the extracellular domains of CD19 interact with the large extracellular loop of CD81, the N terminus and the first transmembrane regions of CD81 are also required for normal CD19 expression (24, 25).

CD81-knockout mice have additional defects in astrocytes, glial cells, retinal pigment epithelium, and oocytes (26–29). In humans, CD81 has been studied with respect to viral and parasite infections.

Conflict of interest: The authors have declared that no conflict of interest exists.
Citation for this article: *J Clin Invest.* 2010;120(4):1265–1374. doi:10.1172/JCI39748.

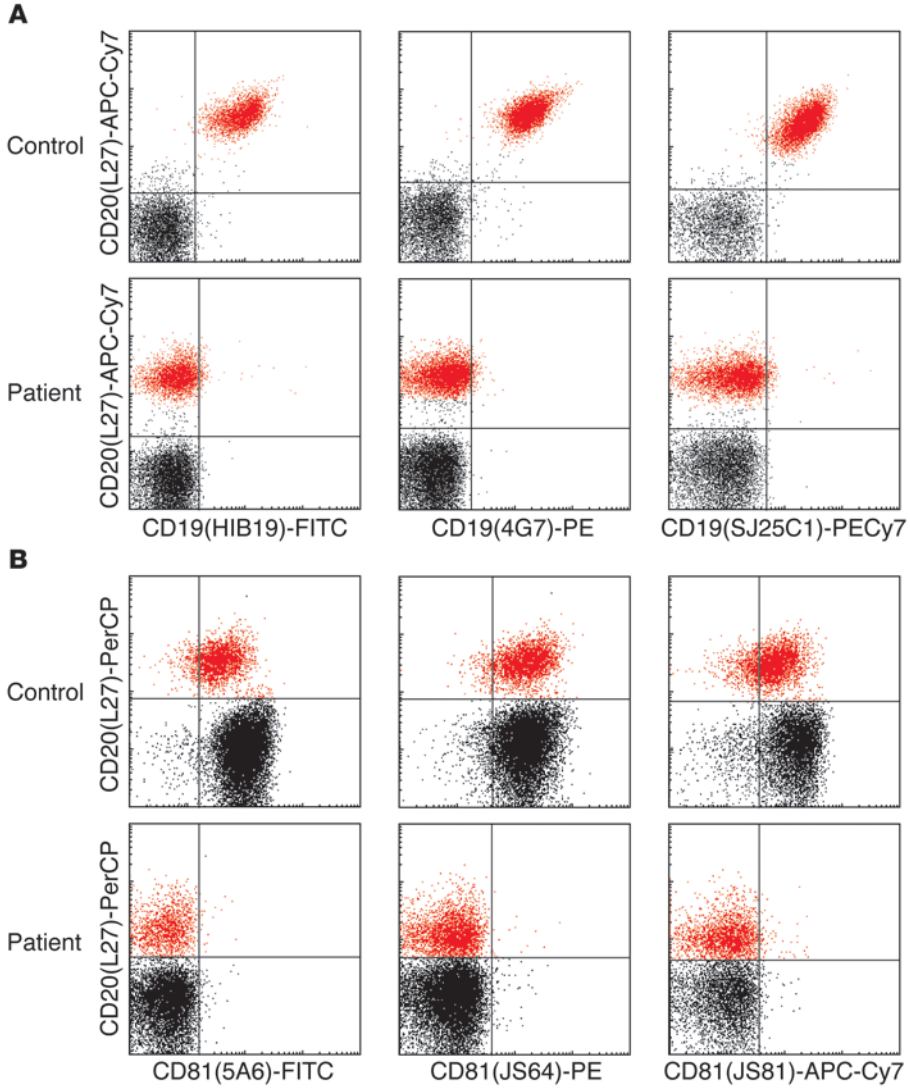

Figure 1
The patient's B cells lack CD19 and CD81 membrane expression. (**A**). Flow cytometric analysis of blood lymphocytes shows the complete absence of CD19 expression on $CD20^+$ B cells from the patient. (**B**). The patient's lymphocytes also completely lack CD81 membrane expression. In all panels, B cells are shown in red and other lymphocytes (mainly T cells and some NK cells) in black. The expression of both CD19 and CD81 was determined with 3 different monoclonal antibodies.

Results

Case report. We evaluated a 6-year-old girl born to consanguineous parents of Moroccan descent who had recurrent respiratory tract infections in the first 2 years of life. At the age of 3.5 years, she developed an acute glomerulonephritis with nephrotic range proteinuria and gross hematuria along with a purpuric rash that appeared on her legs and severe arthralgia. She was admitted by the Nephrology Department at the Queen Fabiola Children's University Hospital in Brussels, Belgium. Clinical examination showed significant hypotrophy (–1 SD for height and weight), a poor general condition, and a distended abdomen with enlarged liver palpable at 2 cm below the rib cage. A renal ultrasound showed bright and enlarged kidneys without hydronephrosis and with a good corticomedullary differentiation. Renal biopsies at the age of 3.5 and 4 years revealed evolutive diffuse endocapillary proliferation in all the glomeruli and the presence of polynuclear cells, fibrinoid necrosis, and extracapillary proliferation with crescents in more than 50% of the glomeruli. Strong mesangial deposition of IgA and C3 was observed with immunofluorescence stainings. A skin biopsy performed at the age of 3.5 showed leukocytoclastic IgA vasculitis. Based on all these data, a diagnosis of Henoch-Schönlein purpura was established, and the girl was treated consecutively with steroid boluses and a 12-week course of oral cyclophosphamide followed by oral steroids (1–2 mg/kg/d) and mycophenolate mofetil and then azathioprine (2 mg/kg/d). Despite treatment, she had ongoing nephrotic-range proteinuria and recurrent episodes of hematuria and evolved progressively to end-stage renal failure within 4 years after her initial presentation and will need renal replacement therapy in the near future. In parallel to the evolution to end-stage renal failure, proteinuria was reduced, and the sedimentation rate and platelet counts normalized.

The child also presented with recurrent episodes of thrombocytopenia associated with antiplatelet antibodies (2.5, with a normal range of 0.01–1) and a persistent inflammatory syndrome with erythrocyte sedimentation rate (ESR) varying between 50 and 80 mm/h. Therefore, at the age of 6 she was referred to the Immunobiology Clinic of the Hôpital Erasme. She was found to be hypogammaglobulinemic, with persistently low IgG concentrations (2.4 g/l) but normal IgM (0.9 g/l) and normal to low IgA serum levels (1.7 g/l at 6 years; 0.59 g/l at 8 years). No antibody recall response was found upon vaccination with both tetanus and pneumococcal antigens, even though the child had been previ-

Both hepatitis C virus and *Plasmodium* sporozoites interact with CD81 to infect hepatocytes (30, 31). Furthermore, it has recently been shown that HIV particle assembly in infected T cells critically depends on CD81 (32). Still, besides an antiproliferative effect in in vitro studies (33), the physiological role of CD81 in humans remains unclear.

We identified a CD19 deficiency in a 6-year-old girl with an antibody deficiency syndrome and glomerulonephritis. The absence of CD19 molecules on the patient's B cells was caused not by a defective *CD19* gene, but by a homozygous *CD81* gene defect. Our studies on this patient show that defects in members of the CD19 signaling complex represent a separate category of antibody deficiencies. To our knowledge, gene defects in *CD81* have not been described before, and therefore careful examination of the patient allowed for the first time study of the physiological and nonredundant functions of CD81 in humans.

Table 1
Lymphocyte subsets in blood from the patient and family members[A]

Lymphocytes (cells/mm^3)	Patient (6 yr)	Father (38 yr)	Mother (39 yr)	Brother (3 yr)	Controls (1–10 yr)
Total lymphocytes	2,195	2,170	2,040	2,249	2,906
CD3$^+$ T cells	1,385	1,253	1,172	1,145	2,000
CD4$^+$ T cells	956	831	745	686	1,247
CD8$^+$ T cells	345	293	383	282	547
CD16/56$^+$ NK cells	292	506	205	326	266
CD20$^+$ B cells	426	269	243	651	453
B cell subsets (CD20$^+$; %)					
CD24^{hi}CD38^{hi}CD27$^-$ transitional	**1**	6	7	14	6
CD24^{dim}CD38^{dim}CD27$^-$ naive mature	**90**	60	47	60	66
CD27$^+$IgM$^+$IgD$^+$ memory	**4**	22	16	17	7
CD27$^+$IgD$^-$ memory	**3**	8	27	7	11
CD5$^+$	**12**	6	33	55	24
T cell subsets (CD4$^+$; %)					
CD25^{hi}CD127$^-$FoxP3$^+$ Treg	3.87	ND	ND	ND	2.81 ± 0.79
IL17$^+$ Th17[B]	0.08	ND	ND	ND	0.18 ± 0.13

[A]Data are shown as mean ± SD, with n = 17 controls for all subsets except T cell subsets, where n= 7. [B]Measured after 24-hour stimulation with SEB; IL-17 concentration in 96-hour SEB-stimulated cell culture supernatants was 553.6 pg/ml (controls, 646.2 ± 176). ND, not determined. Subnormal values are shown in bold.

ously vaccinated. In addition, the child's allohemagglutinin titer (1/4 anti-B; blood group A) was low. Therefore, she was started on monthly infusions of intravenous immunoglobulins.

B and T cell subsets. To study potential causes of the persistent inflammatory syndrome and the antibody deficiency, flow cytometric analysis was performed on peripheral blood of the patient. This showed normal numbers of T, B, and NK cells (Table 1). The frequency of regulatory T cells was within the normal range, and the frequency of Th17 cells was not increased, making a defect in this compartment as a cause for the inflammatory syndrome less likely.

B cells were present at normal levels; however, these all lacked CD19 expression (Figure 1A). Furthermore, within the B cell compartment, the relative frequencies of transitional B cells and memory B cells were reduced (Table 1 and Supplemental Figure 1; supplemental material available online with this article; doi:10.1172/JCI39748DS1).

Homozygous splice site mutation in the CD81 gene. The defects in the B cell compartment resembled those observed in 5 recently described patients with an antibody deficiency due to *CD19* gene mutations (5, 6). However, sequence analysis revealed no mutations in the *CD19* gene of the patient. In fact, she was heterozygous for a common polymorphism, making the CD19 locus an unlikely candidate for the primary defect.

For determination of a likely cause of the CD19 deficiency, attention was focused on CD21, CD81, and CD225, which together with CD19 form a BCR coreceptor complex. The dependency of CD19 expression on CD81 made us consider the latter as prime candidate, and its expression was studied with additional flow cytometric immunophenotyping. CD81 is normally expressed on blood lymphocytes, monocytes, basophilic granulocytes, and eosinophils, and to our knowledge, the absence of CD81 membrane expression has not been reported before in humans. Furthermore, the B cells in all 611 neonatal cord blood samples from the Generation R Study showed CD81 membrane expression (34). However, we were unable to detect any membrane expression of CD81 on leukocytes of the patient (Figure 1B). Therefore, all 8 exons and splice sites were sequenced in genomic DNA of the patient, resulting in the identification of a homozygous G>A substitution directly downstream of exon 6: c.561+1G>A (Figure 2A). Sequencing of *CD81* transcripts revealed 13 additional nucleotides downstream of exon 6, which cause a frameshift and a premature stop (p.Glu188MetfsX13) before the fourth transmembrane domain. Due to the mutation, the splice donor site was disrupted, and a cryptic splice site in intron 6 was used (Figure 2A). Both parents and the younger brother of the patient were heterozygous for the mutation and showed no clinical signs of immunodeficiency (Figure 2B).

CD81 transcript levels. The effect of the *CD81* splice site mutation was studied with 3 real-time quantitative PCR assays detecting *CD81* splice variants in cDNA from PBMCs. Total *CD81* transcript levels of the patient and all 3 carriers were within the range of healthy controls (Figure 2C). Correctly spliced *CD81* transcripts were normally expressed in carriers but not in the patient. In contrast, alternative *CD81* transcripts using the cryptic splice site in intron 6 were highly expressed in the patient and in the carriers, but not in healthy controls. These data show that the mutation does not affect the overall level of *CD81* transcripts. However, the mutation does completely disrupt the splice donor site of exon 6, and the mutated allele only produces alternative splice products. Finally, wild-type *CD81* transcripts were not alternatively spliced.

Expression of CD19 complex members. The mutated *CD81* alleles clearly generated only alternative splice products, which encode hypothetically truncated protein. The effect of the alternatively spliced *CD81* transcripts on membrane of CD81 was studied by flow cytometric immunophenotyping of B cells from carriers and controls. Interestingly, CD81 was consistently reduced on B cells of the carriers as compared with controls, despite the normal levels of wild-type CD81 transcripts (Figure 2D). Apparently, both alleles of *CD81* are required to produce normal protein levels.

The effects of reduced CD81 expression on other members of the CD19 complex were also studied. In addition to the lack of CD19 expression on patient's B cells, CD19 levels were reduced on

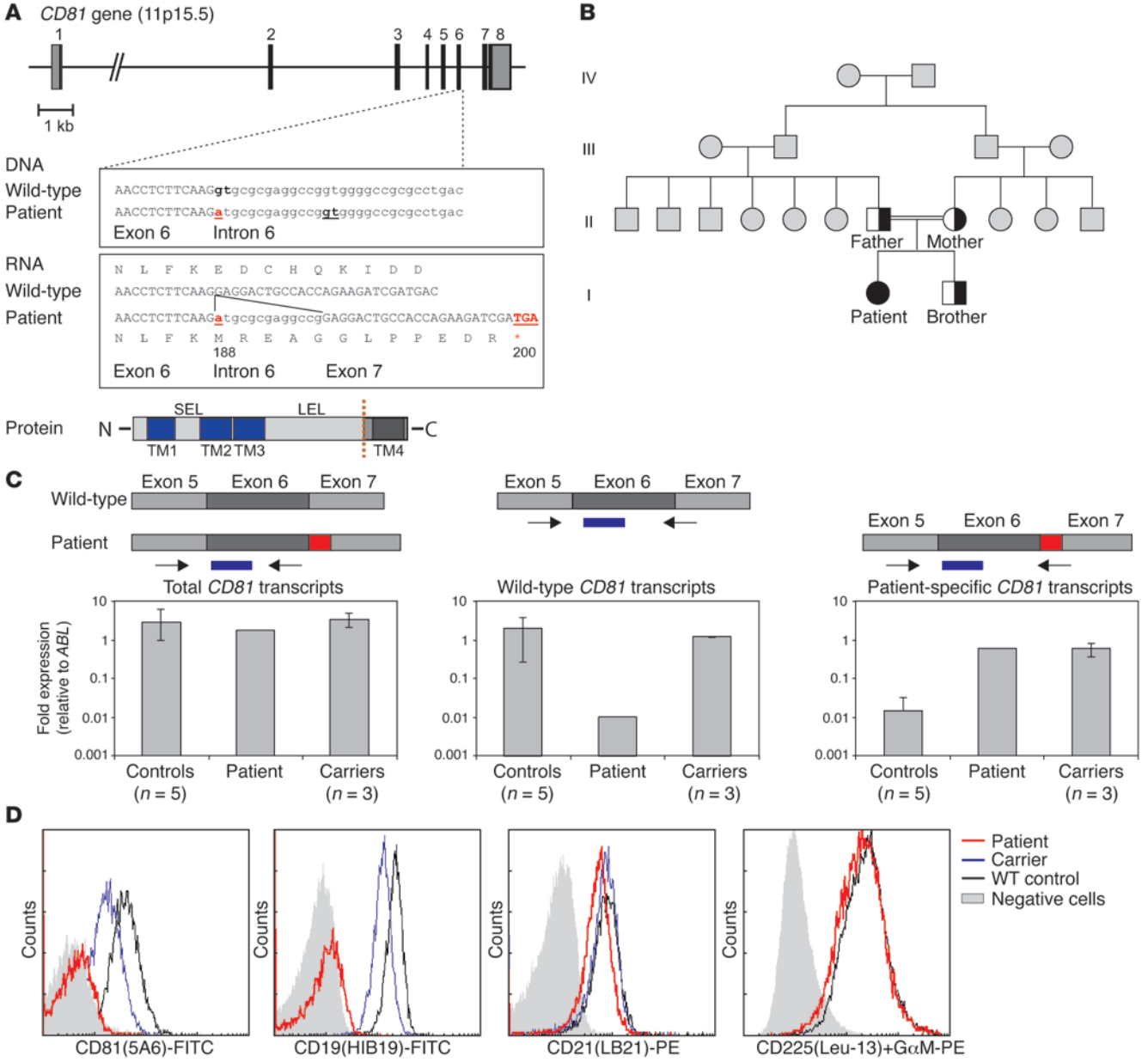

Figure 2

Homozygous *CD81* splice site mutation results in alternative splicing and disruption of the CD19 complex on B cells. (**A**). Schematic representation of the *CD81* gene, consisting of 8 exons. The patient was homozygous for a splice site mutation downstream of exon 6 (exon6+1 G>A) resulting in the use of a cryptic splice site 13 nucleotides downstream of exon 6. The 13-nucleotide insertion results in a frameshift and a premature stop codon upstream of the fourth transmembrane domain of the CD81 protein. TM, transmembrane domain; SEL, short extracellular loop; LEL, large extracellular loop. (**B**). Pedigree of the family of the CD81-deficient patient. Half-filled symbols denote known carriers of the mutation; the filled symbol represents the patient, who is homozygous for the mutation; gray symbols denote family members who were not tested for carriership of the mutation; squares denote male family members; circles denote female family members. The parents of the patient were consanguineous (double line). (**C**). Quantitative analysis of *CD81* transcripts in blood mononuclear cells. Three PCR assays were developed to quantify total, wild-type, and alternatively spliced *CD81* transcripts. Arrows indicate primers; blue bars denote TaqMan probes. Data represent mean ± SD. (**D**). Expression levels of CD19 complex members on B cells of the patient and a carrier of the *CD81* mutation. CD19 and CD81 expression were absent on patient's B cells and reduced in carriers of the mutation. CD21 and CD225 were normally expressed. Isotype controls are shown for CD81 and CD225 stains and CD20-negative lymphocytes for CD19 and CD21 stains.

B cells of all 3 carriers (Figure 2D). CD21 was only slightly reduced on patient's B cells and normally expressed in carriers. Finally, CD225 was found to be normally expressed on EBV-transformed B cells of the patient. These results support the critical role of CD81 in CD19 expression, whereas CD21 and CD225 do not seem to depend heavily on CD81 expression.

In vitro complementation of the CD81 deficiency. To test whether the loss of CD81 and CD19 expression was the direct result of the

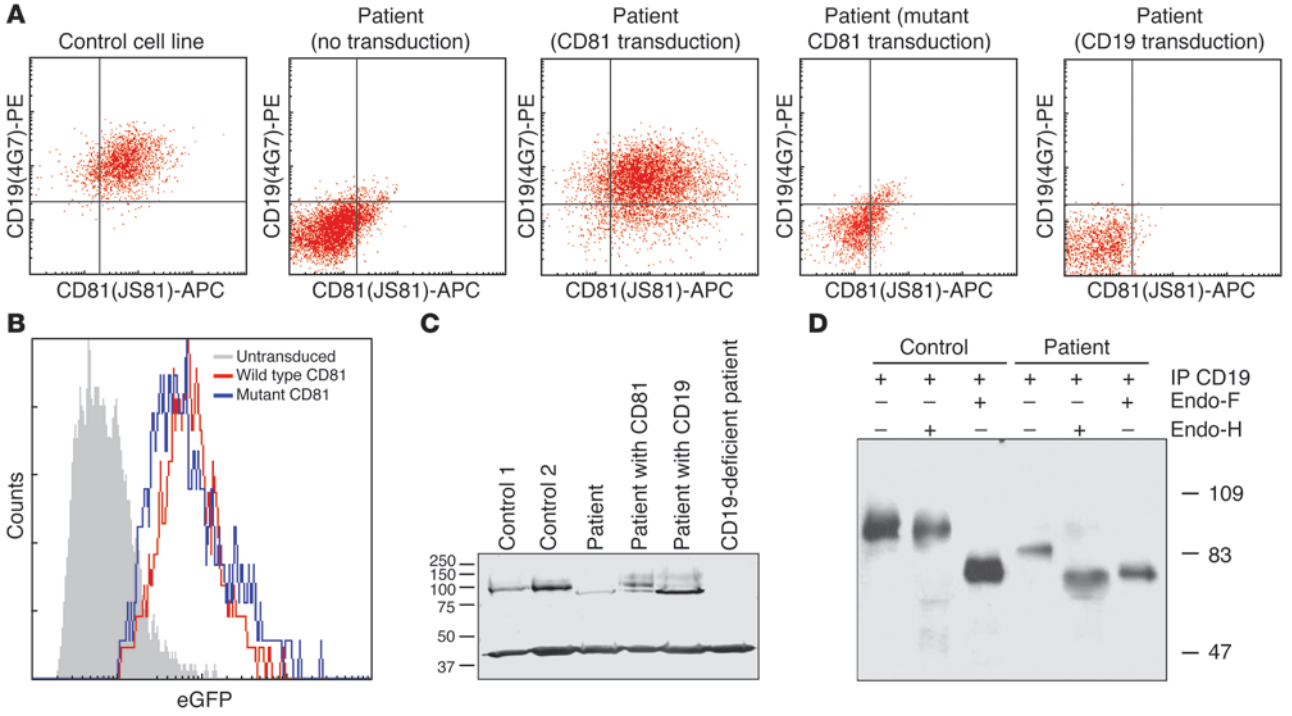

Figure 3

Loss of both CD19 and CD81 membrane expression on the patient's B cells is due to the *CD81* gene defect. (**A**) The expression levels of CD19 and CD81 on EBV-transformed cell lines of the patient, a wild-type control, and patient cells after transduction with wild-type CD81, mutant CD81 (p.Glu188MetfsX13), or wild-type CD19. (**B**) eGFP expression levels in the patient's EBV cells indicate similar expression of the wild-type and mutant CD81 constructs. (**C**) CD19 Western blot of EBV cell lines shows drastically reduced CD19 expression in the patient's B cells. The molecular mass (M_r) of CD19 is lower than in controls and could only be restored upon transduction of CD81 and not CD19. (**D**) Immunoprecipitation followed by digestion with endo-H or endo-F demonstrated that the CD19 molecules in control and patient cells are sensitive to endo-F, and the deglycosylated CD19 molecules migrate similarly. However, only the patient's CD19 is sensitive to endo-H digestion, indicating an ER/pre-Golgi location.

splice site mutation, we transduced EBV-transformed B cells of the patient with retroviral constructs containing wild-type CD81, mutant CD81, or wild-type CD19. Whereas EBV-transformed B cells of a healthy control showed clear expression of both CD81 and CD19, EBV-transformed B cells of the patient lacked CD81 and CD19 expression, similar to freshly isolated B cells (Figure 3A). Upon transduction with wild-type CD81, the patient's EBV-transformed B cells expressed both CD81 and CD19. In contrast, transduction with mutant CD81 did not restore CD81 and CD19 expression, despite similar eGFP expression levels (Figure 3B). Furthermore, wild-type CD19 could not restore membrane expression of either CD19 or CD81. These results show that the patient's B cells are able to produce and express CD19 but that its membrane expression critically depends on wild-type CD81.

To demonstrate that the mutant CD81 underlies the CD19 expression defect, we performed complementation experiments in the U937 leukemic monocyte lymphoma cell line. U937 was dimly positive for staining with CD81 antibody clones 5A6 and JS64 and negative for CD81 clone JS81 (Supplemental Figure 2A) (20, 35). Upon transduction with wild-type CD81, but not with mutant CD81, the expression levels increased enormously (Supplemental Figure 2B). Finally, only wild-type CD81 resulted in high CD19 membrane expression upon cotransduction with wild-type CD19 (Supplemental Figure 2C).

To demonstrate how CD81 regulates CD19 expression, we performed Western blot analysis of EBV cells with a polyclonal CD19 antibody directed against the intracellular domain. Controls showed clear CD19 expression, whereas CD19 was completely absent in EBV B cells from a CD19-deficient patient who lacks the complete intracellular domain (5). In EBV B cells from our CD81-deficient patient, we found strongly reduced CD19 expression with a lower molecular mass (M_r) than in controls. CD81 transduction restored high-M_r CD19 expression, whereas CD19 transduction only increased the levels of low-M_r CD19 (Figure 3C). Membrane CD19 is heavily glycosylated, and the low-M_r CD19 in the patient could be a different glycoform. Therefore, immunoprecipitated CD19 from control and patient EBV B cells was digested with *N*-glycosidase-F (endo-F) or endoglycosidase-H (endo-H). The CD19 molecules from both cell lines were sensitive to endo-F digestion, and the deglycosylated CD19 migrated similarly. However, only the patient's CD19 was sensitive to endo-H digestion, indicating a defect in maturation that retains CD19 in an ER/pre-Golgi location in the absence of wild-type CD81 (Figure 3D) (36–38). From these combined observations, we conclude that in humans, CD19 membrane expression critically depends on wild-type CD81.

Antibody responses. CD19 deficiencies lead to an antibody deficiency syndrome due to a B cell–intrinsic impaired antigen-specific response (5). Since the patient described herein lacked CD19 expression on B cells due to the *CD81* gene defect and was clearly hypogammaglobulinemic, we hypothesized that she would have B cell defects similar to those of the earlier reported CD19-deficient patients (5,

Table 2
Patient's antibody responses upon booster vaccinations

	Before	After[A]	Control values
Ab-secreting cells[B]			
Total IgA	**50**	ND	5,862
Total IgG	**6**	**13**	6,830
Anti–tetanus toxoid IgG	ND	**3**	1,000
Anti-pneumococcus IgG[C]	ND	**0**	630
Serum Ig levels			
Total IgM (g/l)	0.9	–	0.5–1.8
Total IgA (g/l)	1.7	–	0.1–2.0
Total IgG (g/l)	**2.4**	–	4–11
Anti-tetanus toxoid IgG[D] (IU/ml)	0.26	0.34	>0.01
Anti-pneumococcus IgA[C] (IU/ml)	**0**	**0**	>10
Anti-pneumococcus IgG[C,D] (IU/ml)	**3**	**7**	>10
–serotype 1 IgG[D] (μg/ml)	**0.10**	**0.07**	>0.20
–serotype 7 IgG[D] (μg/ml)	**0.16**	**0.15**	>0.20
–serotype 14 IgG[D] (μg/ml)	0.21	**0.13**	>0.20
–serotype 19 IgG[D] (μg/ml)	**0.17**	**0.18**	>0.20
–serotype 23 IgG[D] (μg/ml)	**0.15**	**0.07**	>0.20

[A]Antibody-secreting cells were measured 7 days after the vaccine boosters; serum Ig levels were measured 28 days after the vaccine boosters. [B]Values per 10^6 mononuclear cells are shown. [C]Measured with the Pneumo-23 vaccine [D]Measured after the patient was started on IVIg substitution therapy. Subnormal values are shown in bold.

6). To determine whether the low total and antigen-specific Ig levels resulted from impaired antibody responses, we administered booster vaccinations with tetanus toxoid and pneumococcal antigens to the patient and healthy controls. Whereas 7 days after vaccination this resulted in increased numbers of antigen-specific antibody-secreting cells in peripheral blood of healthy controls, very few tetanus-specific or pneumococcus-specific antibody-secreting cells were found in the patient (Table 2). Furthermore, serum analysis showed reduced anti-pneumococcus antibodies, which were not increased 28 days after booster vaccination (Table 2). No IgA antibody response was detectable, even though this vaccine was reported to induce high IgA antibody responses (39). Anti–tetanus toxoid IgG antibodies were detectable in serum of the patient but did not increase after vaccination (Table 2). The detectable IgG levels were likely the result of previous gammaglobulin administration and not of production by the patient's own B cells. Thus, the patient is unable to mount sufficient IgA and IgG responses to both protein and polysaccharide antigens.

Somatic hypermutation. Although the patient showed impaired antibody responses, few memory B cells and low serum Ig levels were clearly detectable. These signs of immunological memory demonstrate that the antibody deficiency is not absolute. To gain insight into this issue, the somatic hypermutations (SHMs) were studied in VH-Cα and VH-Cγ transcripts of the few blood memory B cells. Most of these transcripts contained SHMs, and their pattern suggested the potential to produce an antigen-selected BCR repertoire. However, the overall mutation frequency in VH gene segments of the analyzed transcripts was significantly lower than in age-matched healthy controls (Figure 4). Thus, in addition to the reduced ability to mount antibody responses, the few responses that had taken place also seemed impaired. Interestingly, SHMs in VH-Cα transcripts of the patient were less severely affected than in VH-Cγ transcripts. This is in line with the reduced IgG levels and normal IgA levels, but not with vaccination responses. Since the patient was unable to mount both IgA and IgG responses, it is likely that the steady-state parameters — IgA levels and SHMs in VH-Cα transcripts — have a different origin.

BCR signaling. The observed defects in antibody responses can potentially result from an intrinsic B cell defect and from defective Th cell responses. Since CD81 and CD19 function in a complex as a coreceptor to the BCR, we first studied BCR signaling by Ca^{2+} influx analysis upon stimulation with anti-IgM independent of T cell help. In contrast to those of healthy controls, the patient's B cells did not show an initial Ca^{2+} flux from the rough endoplasmic reticulum into the cytoplasm (Figure 5). The subsequent sustained influx of extracellular calcium was normal. The defect in stimulation was most likely BCR specific, because in vitro stimulation of naive B cells with CD40L, IL-4, and IL-10 induced similar levels of proliferation and Ig class switching as compared with controls (data not shown) (40). Based on these results, we conclude that CD81-deficient B cells have a specific defect in BCR-mediated stimulation, which underlies, at least in part, the observed impaired antibody responses and consequent impaired memory B cell formation.

T cell responses. To study whether the impaired antibody responses in the CD81-deficient patient also resulted from affected T cell function, we tested in vitro proliferation and IFN-γ production. The patient's lymphocytes showed normal proliferation in response to 3 different mitogens (phytohemagglutinin [PHA], concanavalin A, and pokeweed) and to the candidin antigen (data not shown). This suggests that T cells are intrinsically able to respond properly to antigen.

Furthermore, in in vitro cultures of PBMCs, the patient's T cells produced normal levels of IFN-γ in response to tetanus toxoid 28 days after booster vaccination (Figure 6). In these types of assays, both B cells and monocytes can present antigen to T cells. To determine whether the T cell response was normal upon presentation by B cells, we performed additional experiments with mono-

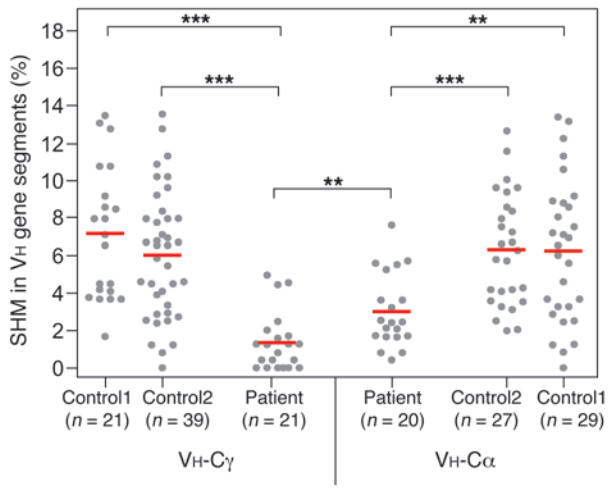

Figure 4
Reduced SHM in VH gene segments of Cα and Cγ transcripts. Sequence analysis revealed significantly reduced SHMs in VH-Cα and VH-Cγ transcripts of the patient as compared with age-matched controls. The frequency of mutations was significantly lower in VH-Cγ transcripts of the patient as compared with VH-Cα transcripts. Individual data points are shown, with red lines denoting mean values. $^{**}P < 0.01$, $^{***}P < 0.001$.

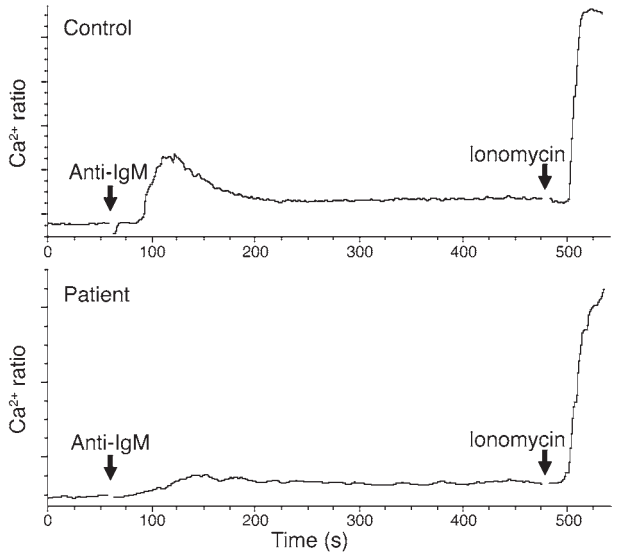

Figure 5
Patient's B cells show an intrinsic defect in signaling upon BCR stimulation. The stimulation of blood mononuclear cells with anti-IgM $F(ab')_2$ fragments did not result in an initial calcium influx in $CD20^+$ B cells from the patient, in contrast to control cells. The subsequent sustained influx of extracellular calcium was normal. No defect in calcium flux was seen in carriers of the *CD81* mutation (data not shown). Ionomycin was added as a control for intracellular loading of Indo-1.

cyte-depleted cultures. In the 3 controls, depletion of monocytes resulted in increased IFN-γ production. However, the patient's T cells tested before and after booster vaccination with tetanus toxoid clearly produced reduced levels of IFN-γ when monocytes were depleted. From this, it was concluded that CD81-deficient B cells were impaired in their ability to support a strong T cell response. A potential explanation is deficient generation of tetanus-specific memory B cells. In healthy controls, these cells recognize, process, and present preferentially tetanus toxoid epitopes, making them highly efficient antigen-presenting cells. The lack of CD81 on T cells does not seem to affect their antigen responses. The antibody deficiency in the patient appears to be the result of a B cell–intrinsic defect in antigen responses and reduced formation of memory B cells and Ig-secreting plasma cells.

Discussion

We report on a patient born to consanguineous parents with a complex clinical picture of progressive nephropathy and profound hypogammaglobulinemia. Due to the consanguinity, multiple recessive genotypes potentially contribute to the severe phenotype. Still, our studies provide clear evidence that the antibody deficiency is the result of a mutation in the *CD81* gene leading to complete lack of CD81 and CD19 membrane expression on B cells and the disruption of the CD19 complex. The antibody deficiency in our patient was remarkably similar to that of patients with CD19 deficiency and was characterized by impaired antibody responses upon vaccination and impaired memory B cell formation, caused by defective activation via the BCR of the CD19- and CD81-negative B cells.

The *CD81* mutation in the patient disrupted a guanine in the highly conserved GT dinucleotide motif of the splice donor site downstream of exon 6 (41). Disruption of this conserved motif completely abrogated normal splicing and induced the use of an alternative splice site. This is in agreement with reported mutations in GT motifs of splice donor sites, which lead to exon skipping or, when present, cryptic splice site utilization (42, 43). Interestingly, total *CD81* transcript levels were normal in the patient, suggesting that the cryptic splice site usage does not overtly affect mRNA formation or RNA stability.

The deficiencies in the B cell compartment of the patient were mostly, but not completely, in agreement with those observed in CD81-knockout mouse models (21–23). Still, the antibody deficiency in our patient seemed more severe, as she also had reduced total serum Ig levels, decreased ex vivo specific IgG and IgA synthesis, and impaired T cell–independent antibody responses. These parameters were all within normal range in CD81-knockout mice (21, 23). A potential explanation is dependence of CD19 on CD81 in B cells from our patient, as shown by the CD19 glycosylation and CD81 reconstitution experiments, whereas the knockout mouse models show residual CD19 expression on B cells (21–23). Furthermore, the patient's B cells were deficient in BCR-mediated signaling, whereas this was normal to high for mouse CD81-deficient B cells (22, 44). It is therefore conceivable that the complete absence of membrane CD19 expression on our patient's B cells underlies the more severe antibody deficiency and thus the difference from the mouse models (21–23).

Serum levels and SHM were not as severely affected for IgA as for IgG in the patient. This is not reflected by the antibody responses upon intramuscular vaccination, because IgA and IgG production were both dramatically reduced in the patient as compared with controls. In contrast to IgG, IgA responses are mostly generated in mucosal tissue. Furthermore, IgA responses can take place outside follicles and can be accomplished by T cell–independent mechanisms, with roles for Toll-like receptor and TACI-dependent signaling (reviewed in ref. 45). These mechanisms might partially compensate for the CD81 deficiency and explain the difference between IgG and IgA memory in the patient.

Besides the intrinsic B cell defects, we did not find evidence for other obvious immunological deficiencies in our patient that could explain the inflammatory syndrome or the antibody deficiency. The T cell, NK cell, and myeloid compartments were overtly normal, as were lymphocyte proliferation and IFN-γ responses. In fact, the only observed defective responses by the patient's T cells were likely to be the result of impaired B cell function and consequent impaired T-B interaction, as was seen in CD81-knockout mouse models (21–23, 46, 47). From this, we concluded that the antibody deficiency results from the CD81 deficiency in the patient's B cells. It remains unclear what cells cause the inflammatory syndrome and whether this is the result of the CD81 deficiency or potential other recessive genotypes.

Abnormalities in brain size and retinal pigment epithelium thickness have been described in CD81-knockout mice but were not detected in our patient. This could indicate a difference between humans and mice in the redundancy of CD81 function in these tissues. However, in mice, these abnormalities depended heavily on the genetic background (26, 29) and require further study when new CD81-deficient patients are identified.

It remains unclear whether the nephropathy in our patient results directly from the *CD81* gene defect. Deficiencies of tetraspanin molecules CD63 and CD151 have been reported to result in kidney pathology in mouse and humans, respectively (48, 49). However, these pathologies were the result of disrupted structural organization of the organ, whereas in the patient described here, IgA deposits seem to underlie the defect. In addition, no kidney problems were

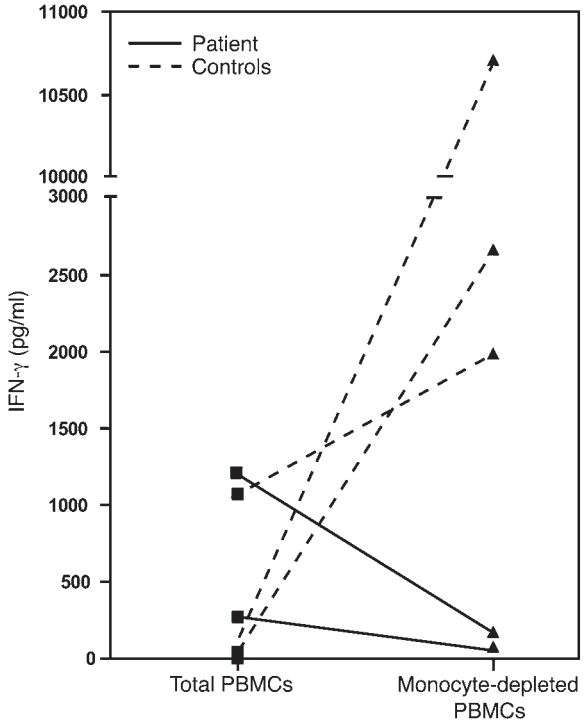

Figure 6
Tetanus toxoid–induced IFN-γ production by total PBMCs compared with monocyte-depleted PBMCs. IFN-γ concentrations were measured by ELISA in the supernatants after 7-day cultures of blood mononuclear cells or monocyte-depleted cell suspensions in the presence of 5 μg/ml tetanus toxoid. In contrast to 3 controls, the patient's responses were decreased when monocytes were depleted before culture. Dotted lines denote healthy controls, and solid lines represent the patient before (lower line) and 1 month after a tetanus toxoid booster (upper line).

reported in 3 independently generated CD81-knockout mouse models (21–23). Henoch-Schönlein purpura nephritis and the related IgA nephropathy can be considered autoimmune diseases, often preceded by infection (reviewed in refs. 50, 51). Some immunogenetic factors have already been identified for these diseases, such as null alleles for complement C4A and C4B (52), but the precise pathogenesis is still not known. It is clearly related to the synthesis of aberrantly glycosylated IgA1, exposing *N*-acetylgalactosamine–containing neoepitopes to naturally occurring IgG and IgA1 antibodies, which results in the formation of immune complexes (53). This IgA is suggested to be of mucosal origin, which could explain why no IgA secretion was detectable by the circulating lymphocytes from the patient (54). Elevated serum secretory IgA levels are reported to be associated with a more severe phenotype of the nephropathy (54). The decreased immunity and increased infection in our patient could have contributed to development of the IgA nephropathy, similar to that in a recently identified CD19-deficient patient (55).

The Henoch-Schönlein purpura nephritis and the recurrent episodes of thrombocytopenia associated with antiplatelet antibodies are 2 autoimmune manifestations. While this seems contradictory in an immunodeficient patient, about 20%–35% of antibody-deficient patients currently classified as CVID show signs of autoimmunity (10, 56). In fact, several CD19-deficient patients have high levels of autoantibodies, either with or without an autoimmune disease (5, 6, 55). It is unclear how genetic defects in *CD19* or *CD81* might lead to increased autoantibody levels. BCR-mediated signaling and Toll-like receptor–mediated signaling in precursor B cells are important for the removal of autoreactive B cell receptors, as patients with genetic defects in *BTK* or *MYD88* have been shown to have increased numbers of B cells carrying autoreactive BCRs (57, 58). Since the CD19 complex is important for signaling via the BCR, it might have a similar function in the removal of autoreactive B cell receptors. Therefore, genetic defects in *CD19* or *CD81* could lead to increased frequencies of autoreactive B cells.

The vast majority of patients with an antibody deficiency of unknown origin are currently classified as having CVID (59). The recent identification of monogenetic defects and risk-associated alleles in CVID patients could support classification into distinct disease categories (4, 5, 7–9). In fact, the antibody deficiency in our patient was highly similar to those observed in CD19-deficient patients, underlining the unique and essential role of the CD19 complex in the human immune system for the generation of strong antigen responses by B cells via dual antigen recognition with the BCR. Therefore, we propose that CD19 complex deficiencies represent a separate disease category within the group of antibody deficiency syndromes. Understanding immunological defects will not only have major implications for the diagnosis and classification of primary antibody deficiencies, but, in particular, enable more specific therapeutic approaches in the future aimed at prevention of irreversible organ damage.

Methods

Diagnostic work-up of blood and vaccinations were carried out with approval of the Commission d'Ethique Médicale of Queen Fabiola Children's Hospital and informed consent of the child's parents.

Flow cytometry. Six-color flow cytometric immunophenotyping of blood samples from the patient, 3 relatives, and 17 control children was performed to analyze leukocyte subsets and protein expression. Furthermore, 611 neonatal cord blood samples from the Generation R Study were analyzed for CD81 expression on B cells (34). Regulatory T cells were identified using CD3-PerCP, CD4-FITC, CD8-APC-H7, CD25-PE-Cy7, CD127-PE (BD Biosciences) and Foxp3-APC (intracellular; eBioscience). Th17 cells were detected after overnight stimulation with SEB (Sigma-Aldrich) using CD3-PerCP, CD4-APC-H7, CD8-PE-Cy7, and IL-17A Alexa Fluor 647 (intracellular; eBioscience). CD225 (Leu-13) was provided by S. Evans, Roswell Park Cancer Institute, Buffalo, New York.

Mutation analysis. All exons of the *CD19* (NCBI AB052799), *CD81* (NCBI EF064749), and *IFITM1* (encoding CD225; NCBI NC_000011) genes were PCR amplified (ref. 5 and Supplemental Table 1) using DNA isolated from post-Ficoll granulocytes of the patient and sequenced on an ABI Prism 3130 XL fluorescence sequencer (Applied Biosystems).

Total cDNA was prepared from mRNA isolated from mononuclear cells of the patient as described previously (60). Fragments of *CD81* cDNA (NCBI NM_004356) were amplified and sequenced to determine the effect of the splice site mutation found in genomic DNA (Supplemental Table 2).

CD81 transcript levels. Three TaqMan real-time quantitative PCR assays were designed to determine transcript levels of total *CD81*, wild-type *CD81*, and patient-specific *CD81* in PBMCs of the patient, 3 carriers, and 5 healthy controls. A common forward primer in exon 5 and a FAM-TAMRA–labeled probe in exon 6 were used against unique reverse primers that were designed in exon 6, on the junction of exons 6 and 7, and on the patient-specific junction including 13 additional nucleotides (Supplemental Table 3). The expression levels were normalized using control gene *ABL* (61). All reactions were run on the ABI Prism 7000 sequence detection system (Applied Biosystems) as described previously (62).

SHM analysis. Hypermutation was studied in VH3-Cα, VH4-Cα, VH3-Cγ, and VH4-Cγ fragments, amplified from PBMC cDNA and cloned into pGEM-T easy vector (Promega). ImMunoGeneTics (IMGT) nomenclature (http://imgt.cines.fr/) was used to assign the V, D, and J segments and to identify somatic mutations (63). The mutation frequency was determined for VH gene segment of each transcript. Furthermore, we studied the replacement/silent (R/S) ratio of these mutations for the framework and the complementarity-determining regions (CDRs), and the distribution of replacement mutations in the framework regions was analyzed according to the binomial distribution model of Chang and Casali (64).

EBV transformation and retroviral transduction. Viral supernatant was collected from the B95-8 cell line (provided by R. Longnecker, Northwestern University, Chicago, Illinois) after incubation at 37°C for 48 hours and stored at –70°C. Post-Ficoll PBMCs were incubated for 1 hour at 37°C with thawed viral supernatant, followed by supplementation with culture medium containing 20% FCS, 2% antibiotics, and 20 μg/ml PHA. After 2–4 weeks, clones started to grow that showed characteristics typical of EBV-transformed B cell lines as determined by flow cytometry.

Wild-type human *CD19* and *CD81* cDNA (Open Biosystems) and mutant *CD81* (PCR-amplified from patient's cDNA) were cloned into retroviral LZRS-IRES-Lyt2a or LZRS-IRES-eGFP vectors. The LZRS-IRES constructs were transfected into the Phoenix amphotropic packaging cell lines using Fugene-6 (Roche Molecular Biochemicals). Stable high-titer producer clones were selected with puromycin (1 μg/ml) (62). The U937 and the EBV-transformed B cell lines were cultured for several days in RPMI 1640 medium containing 10% FCS and antibiotics before transduction using RetroNectin-coated petri dishes (Takara) and recombinant retrovirus containing supernatant for 2 days. Transduced cells were identified by eGFP expression (CD81 constructs) or mouse CD8 expression (Lyt2a; CD19 construct).

Western blotting and immunoprecipitation. Lysates of 10^6 EBV B cells were separated by SDS-PAGE and immunoblotted with the use of a polyclonal rabbit antiserum against the intracellular region of human CD19 (Cell Signaling Technology) and mouse anti-human actin (Abcam). Secondary stains were performed with anti-rabbit IRDye 800CW and anti-mouse IRDye 680 prior to detection on an Odyssey imaging system (LI-COR Biosystems).

Cells (10^8) of the EBV-transformed B cells were lysed 45 minutes on ice in 1 ml 150-mM NaCl, 10 mM Tris-HCl containing 1% Triton-X100, and complete EDTA-free protease inhibitor mixture (Roche Diagnostics), then clarified by centrifugation. Cell lysates were further precleared using protein G immobilized on Sepharose beads (Sigma-Aldrich). CD19 was immunoprecipitated overnight from the precleared lysates using goat anti-mouse IgG Dynabeads (Invitrogen) preloaded with 30 μg mouse anti-human CD19 (clone 4G7), followed by washing in PBS. The immunoprecipitated CD19 was eluted in 100 μl glycoprotein denaturing buffer (New England Biolabs) by boiling for 5 minutes. Eluted CD19 was then digested with either endo-H or endo-F (New England Biolabs) to cleave all N-glycans or left undigested. Samples derived from about 1.5×10^6 cells were loaded per well of a 4%–12% SDS-PAGE, then subjected to Western blotting using a rabbit anti-CD19 polyclonal antibody (Cell Signaling Technology) and detected by a goat anti-rabbit Ig-HRP (Biosource International).

B cell receptor stimulation and Ca^{2+} flux analysis. PBMCs were incubated with 6 μg/ml Indo-1 (Molecular Probes, Invitrogen) and used to evaluate the Ca^{2+} fluxes upon BCR stimulation (5). Free intracellular Ca^{2+} concentrations were determined in CD20-positive B lymphocytes by flow cytometry using a FACSVantage station (BD Biosciences) before and after stimulation with 20 μg/ml goat anti-human IgM-F(ab′)$_2$ (Jackson ImmunoResearch Laboratories Inc.). Subsequently, 2 μg/ml ionomycin (Molecular Probes) was added after each response to control for intracellular loading of Indo-1.

Antigen-specific antibody responses. Serum anti–tetanus toxoid IgG levels and anti-pneumococcal IgG and IgA levels were measured before and 4 weeks after booster vaccinations by ELISA methods as previously described (39, 65, 66).

The numbers of circulating immunoglobulin-secreting cells were measured by ELISPOT as previously described with slight modifications (39). Briefly, ELISPOT plates were coated with 25 μg/ml pneumococcal capsular polysaccharides (Pneumo 23, Sanofi Pasteur MSD) or tetanus toxoid (Statens Serum Institut) or with 10 μg/ml goat anti–human IgG and goat anti–human IgA (SouthernBiotech). Blood mononuclear cells were processed in the ELISPOT plates immediately after isolation. After incubation overnight, filtered AP-conjugated goat anti–human IgG (1:10,000; SouthernBiotech) was added for 2 hours at 37°C. After 5 washes with PBS-Tween 0.5% and 1 with PBS, filtered BCIP/NBT^{plus} (Moss Inc.) was added, and the reaction was stopped with tap water when spots appeared. Spots were counted using an inverted microscope and recorded as the number of immunoglobulin-secreting cells (ISCs) per 10^6 blood mononuclear cells.

In vitro T cell responses. Lymphocyte proliferation was evaluated after culture in the presence of mitogens for 3 days (PHA, concanavalin A, and pokeweed mitogen) or antigen for 6 days (tetanus toxoid [5 μg/ml; Statens Serum Institut] or candidin [5 IU/ml; Stallergenes]). [^{3}H]thymidine was added during the last 16 hours of the culture to evaluate DNA synthesis.

IFN-γ concentrations were measured by ELISA in the supernatants after 7-day cultures of blood mononuclear cells or monocyte-depleted cell suspensions in the presence of 5 μg/ml tetanus toxoid. Monocyte depletion was performed using RosetteSep (StemCell Technologies) according to the manufacturer's recommendations, and flow cytrometric analysis was performed to assess purity of the depleted fraction.

Statistics. Differences in SHM frequencies were analyzed with the non-parametric Mann-Whitney *U* test (exact test; 2-tailed; $P < 0.05$ was considered significant) in GraphPad Prism 5.0 (GraphPad Software).

Acknowledgments

The authors are indebted to B.A.C. van Turnhout, G.M. Dingjan, E.F.E. de Haas, M. Ducarme, J. Tresnie, V. Verscheure, and S. Giezen for technical support; to W.M. Comans-Bitter for assistance with preparing the figures; to S. Evans at Roswell Park Cancer Institute for providing the CD225 antibody; to R. Longnecker at Northwestern University, Chicago, Illinois, for the B95-8 EBV producer line; and to B.E. Clausen for critical reading of the manuscript. This work was supported by a grant from the Erasmus University Rotterdam (EUR-Fellowship) to M.C. van Zelm and a VENI grant (916.56.107) from the Dutch Organization for Scientific Research (NOW/ZonMW) to M. van der Burg.

Received for publication June 3, 2009, and accepted in revised form January 13, 2010.

Address correspondence to: Jacques J.M. van Dongen, Department of Immunology, Unit Molecular Immunology, Erasmus MC, University Medical Center Rotterdam, Dr. Molewaterplein 50, 3015 GE Rotterdam, Netherlands. Phone: 31.10.7044094; Fax: 31.10.7044731; E-mail: j.j.m.vandongen@erasmusmc.nl.

1. Pan-Hammarstrom Q, Hammarstrom L. Antibody deficiency diseases. *Eur J Immunol*. 2008; 38(2):327–333.
2. Conley ME, et al. Primary B cell immunodeficiencies: comparisons and contrasts. *Annu Rev Immunol*. 2009;27:199–227.
3. Geha RS, et al. Primary immunodeficiency diseases: an update from the International Union of Immunological Societies Primary Immunodeficiency Diseases Classification Committee. *J Allergy Clin Immunol*. 2007;120(4):776–794.
4. Grimbacher B, et al. Homozygous loss of ICOS is associated with adult-onset common variable immunodeficiency. *Nat Immunol*. 2003;4(3):261–268.
5. van Zelm MC, et al. An antibody-deficiency syn-

drome due to mutations in the CD19 gene. *N Engl J Med*. 2006;354(18):1901–1912.
6. Kanegane H, et al. Novel mutations in a Japanese patient with CD19 deficiency. *Genes Immun*. 2007;8(8):663–670.
7. Salzer U, et al. Mutations in TNFRSF13B encoding TACI are associated with common variable immunodeficiency in humans. *Nat Genet*. 2005;37(8):820–828.
8. Castigli E, et al. TACI is mutant in common variable immunodeficiency and IgA deficiency. *Nat Genet*. 2005;37(8):829–834.
9. Sekine H, et al. Role for Msh5 in the regulation of Ig class switch recombination. *Proc Natl Acad Sci U S A*. 2007;104(17):7193–7198.
10. Chapel H, et al. Common variable immunodeficiency disorders: division into distinct clinical phenotypes. *Blood*. 2008;112(2):277–286.
11. Cunningham-Rundles C. Autoimmune manifestations in common variable immunodeficiency. *J Clin Immunol*. 2008;28(suppl 1):S42–S45.
12. Lopes-da-Silva S, Rizzo LV. Autoimmunity in common variable immunodeficiency. *J Clin Immunol* 2009;28(suppl 1):S46–S55.
13. Chua I, Quinti I, Grimbacher B. Lymphoma in common variable immunodeficiency: interplay between immune dysregulation, infection and genetics. *Curr Opin Hematol*. 2008;15(4):368–374.
14. Fearon DT, Carroll MC. Regulation of B lymphocyte responses to foreign and self-antigens by the CD19/CD21 complex. *Annu Rev Immunol*. 2000;18:393–422.
15. Carter RH, Fearon DT. CD19: lowering the threshold for antigen receptor stimulation of B lymphocytes. *Science*. 1992;256(5053):105–107.
16. van Noesel CJ, Lankester AC, van Lier RA. Dual antigen recognition by B cells. *Immunol Today*. 1993;14(1):8–11.
17. Matsumoto AK, et al. Intersection of the complement and immune systems: a signal transduction complex of the B lymphocyte-containing complement receptor type 2 and CD19. *J Exp Med*. 1991;173(1):55–64.
18. Bradbury LE, Kansas GS, Levy S, Evans RL, Tedder TF. The CD19/CD21 signal transducing complex of human B lymphocytes includes the target of antiproliferative antibody-1 and Leu-13 molecules. *J Immunol*. 1992;149(9):2841–2850.
19. Wang Y, et al. The physiologic role of CD19 cytoplasmic tyrosines. *Immunity*. 2002;17(4):501–514.
20. Levy S, Todd SC, Maecker HT. CD81 (TAPA-1): a molecule involved in signal transduction and cell adhesion in the immune system. *Annu Rev Immunol*. 1998;16:89–109.
21. Maecker HT, Levy S. Normal lymphocyte development but delayed humoral immune response in CD81-null mice. *J Exp Med*. 1997;185(8):1505–1510.
22. Miyazaki T, Muller U, Campbell KS. Normal development but differentially altered proliferative responses of lymphocytes in mice lacking CD81. *EMBO J*. 1997;16(14):4217–4225.
23. Tsitsikov EN, Gutierrez-Ramos JC, Geha RS. Impaired CD19 expression and signaling, enhanced antibody response to type II T independent antigen and reduction of B-1 cells in CD81-deficient mice. *Proc Natl Acad Sci U S A*. 1997;94(20):10844–10849.
24. Bradbury LE, Goldmacher VS, Tedder TF. The CD19 signal transduction complex of B lymphocytes. Deletion of the CD19 cytoplasmic domain alters signal transduction but not complex formation with TAPA-1 and Leu 13. *J Immunol*. 1993;151(6):2915–2927.
25. Shoham T, Rajapaksa R, Kuo CC, Haimovich J, Levy S. Building of the tetraspanin web: distinct structural domains of CD81 function in different cellular compartments. *Mol Cell Biol*. 2006;26(4):1373–1385.
26. Geisert EE Jr, et al. Increased brain size and glial cell number in CD81-null mice. *J Comp Neurol*. 2002;453(1):22–32.
27. Kelic S, Levy S, Suarez C, Weinstein DE. CD81 regulates neuron-induced astrocyte cell-cycle exit. *Mol Cell Neurosci*. 2001;17(3):551–560.
28. Rubinstein E, et al. Reduced fertility of female mice lacking CD81. *Dev Biol*. 2006;290(2):351–358.
29. Song BK, Levy S, Geisert EE Jr. Increased density of retinal pigment epithelium in cd81–/– mice. *J Cell Biochem*. 2004;92(6):1160–1170.
30. Cormier EG, et al. CD81 is an entry coreceptor for hepatitis C virus. *Proc Natl Acad Sci U S A*. 2004;101(19):7270–7274.
31. Silvie O, et al. Hepatocyte CD81 is required for Plasmodium falciparum and Plasmodium yoelii sporozoite infectivity. *Nat Med*. 2003;9(1):93–96.
32. Grigorov B, et al. A role for CD81 on the late steps of HIV-1 replication in a chronically infected T cell line. *Retrovirology*. 2009;6:28.
33. Takahashi S, Doss C, Levy S, Levy R. TAPA-1, the target of an antiproliferative antibody, is associated on the cell surface with the Leu-13 antigen. *J Immunol*. 1990;145(7):2207–2213.
34. Duijts L, et al. Fetal growth influences lymphocyte subset counts at birth: the Generation R Study. *Neonatology*. 2008;95(2):149–156.
35. Fritzsching B, et al. Release and intercellular transfer of cell surface CD81 via microparticles. *J Immunol*. 2002;169(10):5531–5537.
36. Helenius A, Aebi M. Intracellular functions of N-linked glycans. *Science*. 2001;291(5512):2364–2369.
37. Ellgaard L, Molinari M, Helenius A. Setting the standards: quality control in the secretory pathway. *Science*. 1999;286(5446):1882–1888.
38. Shoham T, et al. The tetraspanin CD81 regulates the expression of CD19 during B cell development in a postendoplasmic reticulum compartment. *J Immunol*. 2003;171(8):4062–4072.
39. Mascart-Lemone F, et al. Differential effect of human immunodeficiency virus infection on the IgA and IgG antibody responses to pneumococcal vaccine. *J Infect Dis*. 1995;172(5):1253–1260.
40. Tangye SG, Ferguson A, Avery DT, Ma CS, Hodgkin PD. Isotype switching by human B cells is division-associated and regulated by cytokines. *J Immunol*. 2002;169(8):4298–4306.
41. Mount SM. A catalogue of splice junction sequences. *Nucleic Acids Res*. 1982;10(2):459–472.
42. Krawczak M, Reiss J, Cooper DN. The mutational spectrum of single base-pair substitutions in mRNA splice junctions of human genes: causes and consequences. *Hum Genet*. 1992;90(1-2):41–54.
43. Krawczak M, et al. Single base-pair substitutions in exon-intron junctions of human genes: nature, distribution, and consequences for mRNA splicing. *Hum Mutat*. 2007;28(2):150–158.
44. Sanyal M, Fernandez R, Levy S. Enhanced B cell activation in the absence of CD81. *Int Immunol*. 2009;21(11):1225–1237.
45. Cerutti A. The regulation of IgA class switching. *Nat Rev Immunol*. 2008;8(6):421–434.
46. Deng J, Dekruyff RH, Freeman GJ, Umetsu DT, Levy S. Critical role of CD81 in cognate T-B cell interactions leading to Th2 responses. *Int Immunol*. 2002;14(5):513–523.
47. Maecker HT, Do MS, Levy S. CD81 on B cells promotes interleukin 4 secretion and antibody production during T helper type 2 immune responses. *Proc Natl Acad Sci U S A*. 1998;95(5):2458–2462.
48. Schroder J, et al. Deficiency of the tetraspanin CD63 associated with kidney pathology but normal lysosomal function. *Mol Cell Biol*. 2009;29(4):1083–1094.
49. Karamatic Crew V, et al. CD151, the first member of the tetraspanin (TM4) superfamily detected on erythrocytes, is essential for the correct assembly of human basement membranes in kidney and skin. *Blood*. 2004;104(8):2217–2223.
50. Davin JC, Ten Berge IJ, Weening JJ. What is the difference between IgA nephropathy and Henoch-Schonlein purpura nephritis? *Kidney Int*. 2001;59(3):823–834.
51. Sanders JT, Wyatt RJ. IgA nephropathy and Henoch-Schonlein purpura nephritis. *Curr Opin Pediatr*. 2008;20(2):163–170.
52. McLean RH, Wyatt RJ, Julian BA. Complement phenotypes in glomerulonephritis: increased frequency of homozygous null C4 phenotypes in IgA nephropathy and Henoch-Schonlein purpura. *Kidney Int*. 1984;26(6):855–860.
53. Novak J, et al. IgA nephropathy and Henoch-Schoenlein purpura nephritis: aberrant glycosylation of IgA1, formation of IgA1-containing immune complexes, and activation of mesangial cells. *Contrib Nephrol*. 2007;157:134–138.
54. Zhang JJ, Xu LX, Liu G, Zhao MH, Wang HY. The level of serum secretory IgA of patients with IgA nephropathy is elevated and associated with pathological phenotypes. *Nephrol Dial Transplant*. 2008;23(1):207–212.
55. Fieschi C, et al. Complete CD19 deficiency in two patients previously diagnosed as common variable immunodeficiency [abstract]. *Clin Exp Immunol*. 2008;154:222–223.
56. Cunningham-Rundles C, Bodian C. Common variable immunodeficiency: clinical and immunological features of 248 patients. *Clin Immunol*. 1999;92(1):34–48.
57. Isnardi I, et al. IRAK-4- and MyD88-dependent pathways are essential for the removal of developing autoreactive B cells in humans. *Immunity*. 2008;29(5):746–757.
58. Ng YS, Wardemann H, Chelnis J, Cunningham-Rundles C, Meffre E. Bruton's tyrosine kinase is essential for human B cell tolerance. *J Exp Med*. 2004;200(7):927–934.
59. Notarangelo L, et al. Primary immunodeficiency diseases: an update from the International Union of Immunological Societies Primary Immunodeficiency Diseases Classification Committee Meeting in Budapest, 2005. *J Allergy Clin Immunol*. 2006;117(4):883–896.
60. van Dongen JJ, et al. Standardized RT-PCR analysis of fusion gene transcripts from chromosome aberrations in acute leukemia for detection of minimal residual disease. Report of the BIOMED-1 Concerted Action: investigation of minimal residual disease in acute leukemia. *Leukemia*. 1999;13(12):1901–1928.
61. Beillard E, et al. Evaluation of candidate control genes for diagnosis and residual disease detection in leukemic patients using 'real-time' quantitative reverse-transcriptase polymerase chain reaction (RQ-PCR) — a Europe against cancer program. *Leukemia*. 2003;17(12):2474–2486.
62. van Zelm MC, Szczepanski T, van der Burg M, van Dongen JJ. Replication history of B lymphocytes reveals homeostatic proliferation and extensive antigen-induced B cell expansion. *J Exp Med*. 2007;204(3):645–655.
63. Lefranc MP. IMGT databases, web resources and tools for immunoglobulin and T cell receptor sequence analysis, http://imgt.cines.fr. *Leukemia*. 2003;17(1):260–266.
64. Chang B, Casali P. The CDR1 sequences of a major proportion of human germline Ig VH genes are inherently susceptible to amino acid replacement. *Immunol Today*. 1994;15(8):367–373.
65. Stubbe M, Swinnen R, Crusiaux A, Mascart F, Lheureux PE. Seroprotection against tetanus in patients attending an emergency department in Belgium and evaluation of a bedside immunotest. *Eur J Emerg Med*. 2007;14(1):14–24.
66. Tuerlinckx D, et al. Optimal assessment of the ability of children with recurrent respiratory tract infections to produce anti-polysaccharide antibodies. *Clin Exp Immunol*. 2007;149(2):295–302.